

## Higgs couplings and properties

---

**Luca Cadamuro\*** on behalf of the ATLAS and CMS Collaborations

*University of Florida*

*E-mail:* [luca.cadamuro@cern.ch](mailto:luca.cadamuro@cern.ch)

The ATLAS and CMS Collaborations are performing an extensive study of the Higgs boson properties and couplings thanks to the unprecedented possibilities offered by the LHC Run 2 dataset. The Higgs boson mass and width, its couplings, and the production cross section in several kinematic regions are studied with the combination of different production modes and decay channels. This document reviews the current status of these measurements and the prospects for the high-luminosity LHC.

*7th Annual Conference on Large Hadron Collider Physics - LHCP2019*

*20-25 May, 2019*

*Puebla, Mexico*

---

\*Speaker.

## 1. Introduction

The scalar sector represents the cornerstone of the standard model of particle physics (SM). By postulating the existence of a scalar field subject to a potential with a non-zero vacuum expectation value, the Brout-Englert-Higgs mechanism [1, 2] predicts a spontaneous breaking of the electroweak symmetry, thus explaining the origin of the mass of the W and Z bosons and regularising the theory at the TeV scale. Moreover, fermion masses are explained with the introduction of a Yukawa interaction with their corresponding fields. The manifestation of the scalar sector of the SM is the existence of the Higgs boson (H), i.e. the quantum of the field, and its study is one of the priorities of the research programme of the CERN LHC.

An extensive study of the properties and couplings of the Higgs boson is being performed by the ATLAS [3] and CMS [4] Collaborations at the CERN LHC. In particular, the large dataset collected during the LHC Run 2 operations represents an unprecedented possibility for precision Higgs boson measurements. This document focuses on the latest experimental results, obtained with the datasets collected at  $\sqrt{s} = 13\text{ TeV}$  in 2016 (about  $36\text{ fb}^{-1}$ ), 2017 (about  $44\text{ fb}^{-1}$ ) and 2018 (about  $60\text{ fb}^{-1}$ ) operations.

## 2. Mass and width

The mass of the Higgs boson ( $m_H$ ) represents a fundamental parameter of the SM and its measurement fully determines the properties of the scalar sector. The value of  $m_H$  is measured in the two high-resolution decay channels  $H \rightarrow \gamma\gamma$  and  $H \rightarrow ZZ^* \rightarrow 4\ell$ . The precision of the measurement crucially relies on the performance in the determination of the photon and lepton energy scales. Figure 1 reports a summary of the result obtained by the ATLAS Collaboration in the combination of the two decay channels with the Run 1 and Run 2 2016 datasets [5], and the CMS result in the four lepton channel with the Run 2 2016 dataset [6]. The measured values of  $m_H$  are:

Experiment	Measurement	(Stat.	Syst.)	Channel and dataset
ATLAS	$m_H = 124.97 \pm 0.24\text{ GeV}$	$(\pm 0.16$	$\pm 0.18)$	$4\ell + \gamma\gamma$ , Run 1 + Run 2 (2016)
CMS	$m_H = 125.26 \pm 0.21\text{ GeV}$	$(\pm 0.20$	$\pm 0.08)$	$4\ell$ , Run 2 (2016)

The value of  $m_H$  is thus known to a precision of about 2 per mille, still dominated by statistical uncertainties in the four lepton channel.

The SM predicts a width of the Higgs boson ( $\Gamma_H$ ) of about 4 MeV, out of the direct reach of the experiments. However, an indirect constraint on  $\Gamma_H$  can be derived by comparing the on-shell and off-shell cross sections of the  $gg \rightarrow H \rightarrow ZZ^*$  process. Because of the interference of Higgs boson production with the background processes, the ratio of these two quantities directly depends on the Higgs boson width, under the model-dependent assumption of identical on-shell and off-shell coupling modifiers.

The ATLAS Collaboration has derived constraints in both the  $4\ell$  and  $2\ell 2\nu$  channels with the Run 2 2016 dataset [7], while the CMS Collaboration used the  $4\ell$  channel only, combining the Run 1 and Run 2 2016 and 2017 measurements [8]. The upper limits derived by the two experiments at the 95% confidence level are:

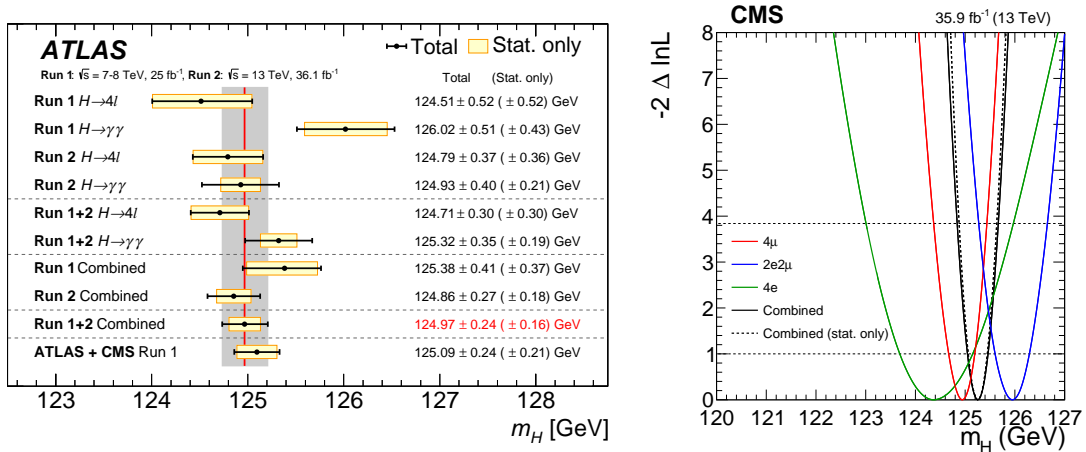


Figure 1: Left: summary of the measured Higgs boson mass values in the  $4\ell$  and  $\gamma\gamma$  final states by the ATLAS Collaboration [5]. Right: negative log-likelihood as a function of the Higgs boson mass for the CMS measurement in the  $4\ell$  decay channel [6].

Experiment	Observed	Expected	$ZZ^*$ decay channel and dataset
ATLAS	$\Gamma_H < 14.4 \text{ MeV}$	$\Gamma_H < 15.2 \text{ MeV}$	$4\ell + 2\ell 2\nu$ , Run 2 (2016)
CMS	$\Gamma_H < 9.16 \text{ MeV}$	$\Gamma_H < 13.7 \text{ MeV}$	$4\ell$ , Run 1 + Run 2 (2016 + 2017)

Figure 2 shows the negative log-likelihood scans as functions of  $\Gamma_H$  for the ATLAS and CMS measurements. In particular, it can be observed from the CMS result that the experimental measurements are starting to set a lower bound on  $\Gamma_H$ , complementing direct searches based on the Higgs boson lifetime measurement [9].

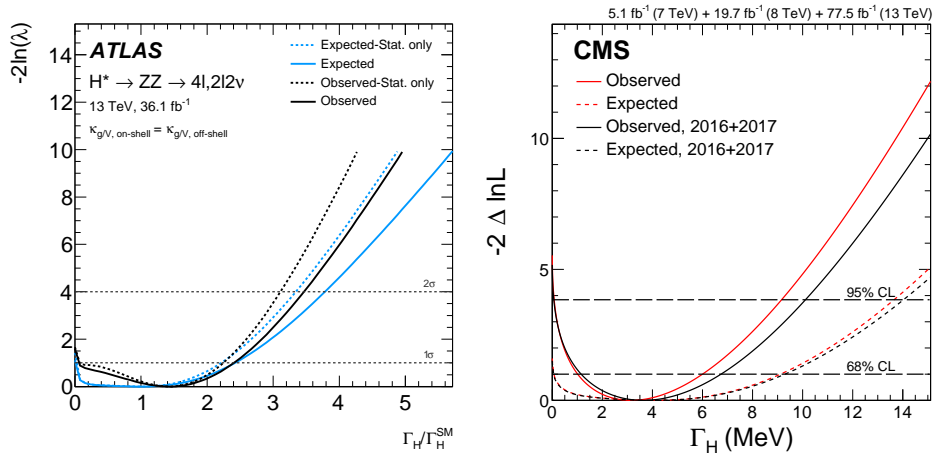


Figure 2: Negative log-likelihood profile as a function of the Higgs boson width for the ATLAS combined measurement in the  $4\ell$  and  $2\ell 2\nu$  final states [7] (left) and for the CMS measurement in the  $4\ell$  final state [8] (right).

### 3. Signal strength and coupling measurements

A global view of the Higgs boson interactions with bosons and fermions is obtained by studying the production cross sections in several modes and exploring different decay channels. The ATLAS and CMS Collaborations have combined the measurements in the  $\gamma\gamma$ ,  $ZZ^*$ ,  $WW^*$ ,  $\tau\tau$ , and  $bb$  decay channels studying the production modes by gluon (ggF) and vector boson (VBF) fusion, and in associated production with a vector boson (VH) and top quark pairs ( $t\bar{t}H$ ) [10, 11]. For each individual production mode  $i$  and decay channel  $f$ , a signal strength  $\mu_i^f$  is defined as the ratio of the measured cross section times branching fraction to the prediction of the SM. This represents the most generic parametrisation per production and decay mode, and the corresponding result is summarised in Fig. 3 by the measurement performed by the ATLAS Collaboration. It can be noticed how both the experimental and theoretical systematic uncertainties have approximately the same magnitude as statistical ones. For a global signal strength  $\mu$  that affects simultaneously all the production and decay modes, the measured values are  $\mu = 1.11_{-0.08}^{+0.09}$  (ATLAS, 2016 and 2017 dataset) and  $\mu = 1.17 \pm 0.10$  (CMS, 2016 dataset).

Signal strengths per production and decay modes can also be defined by introducing a common parameter for different measurements, as shown in Fig. 4. It can be observed how systematic uncertainties are either dominant or at the same level of the statistical uncertainties in all the production and decay modes, with the exception of the signal strength of the  $H \rightarrow \mu\mu$  process.

Signal strength measurements can be interpreted to derive constraints on the Higgs boson couplings. This is done in the context of the  $\kappa$ -framework, introducing a set of parameters that modify the strength of the tree level Higgs boson couplings to the different particles. For Higgs production initiated by  $i$  and decaying into  $f$ , i.e.  $i \rightarrow H \rightarrow f$ , these parameters can be defined from the production cross section and partial decay width as  $\kappa_i^2 = \sigma_i/\sigma_i^{\text{SM}}$  and  $\kappa_f^2 = \Gamma_f/\Gamma_f^{\text{SM}}$ , with the Higgs boson total width also modified consequently by  $\kappa_H^2 = \sum \Gamma_f / \sum \Gamma_f^{\text{SM}}$ . Therefore:

$$\sigma \times \mathcal{B}(i \rightarrow H \rightarrow f) = \frac{\sigma_i \times \Gamma_f}{\Gamma_H} = \frac{\sigma_i^{\text{SM}} \times \Gamma_f^{\text{SM}}}{\Gamma_H^{\text{SM}}} \times \left( \frac{\kappa_i^2 \kappa_f^2}{\kappa_H^2} \right) \quad (3.1)$$

In case of loop-induced processes, individual  $\kappa$  can also be resolved in terms of the modifiers of the couplings to SM particles. In this case, assuming that there are no extra particles in the loops of the processes considered, coupling modifiers can be defined either separately for each particle or with a common modifier for fermions ( $\kappa_F$ ) and bosons ( $\kappa_V$ ). The result is illustrated in Fig. 5. Alternatively, additional degrees of freedom can be added to the tree level couplings to parametrise the effects of physics beyond the SM (BSM), as illustrated in Fig. 6. Effective gluon and photon interactions  $\kappa_g$  and  $\kappa_\gamma$  are defined to parametrise the effects of BSM particles in the loops. Branching fractions are also considered for invisible ( $\mathcal{B}_{\text{inv}}$ , for missing transverse momentum signatures) and undetectable particles ( $\mathcal{B}_{\text{undet}}$ , for signatures where no current experimental sensitivity exists). The values of  $\mathcal{B}_{\text{inv}}$  and  $\mathcal{B}_{\text{undet}}$  are either considered separately or together as a single parameter  $\mathcal{B}_{\text{BSM}} = \mathcal{B}_{\text{inv}} + \mathcal{B}_{\text{undet}}$ . To compensate for the extra degrees of freedom, additional constraints are introduced by requiring  $\mathcal{B}_{\text{BSM}} = 0$  (black line),  $\kappa_V < 1$  (red line), or by adding off-shell cross section measurements with the same modifier as the on shell measurements  $\kappa_{\text{on}} = \kappa_{\text{off}}$  (black line). Compatibility with the SM hypothesis is observed in all cases.

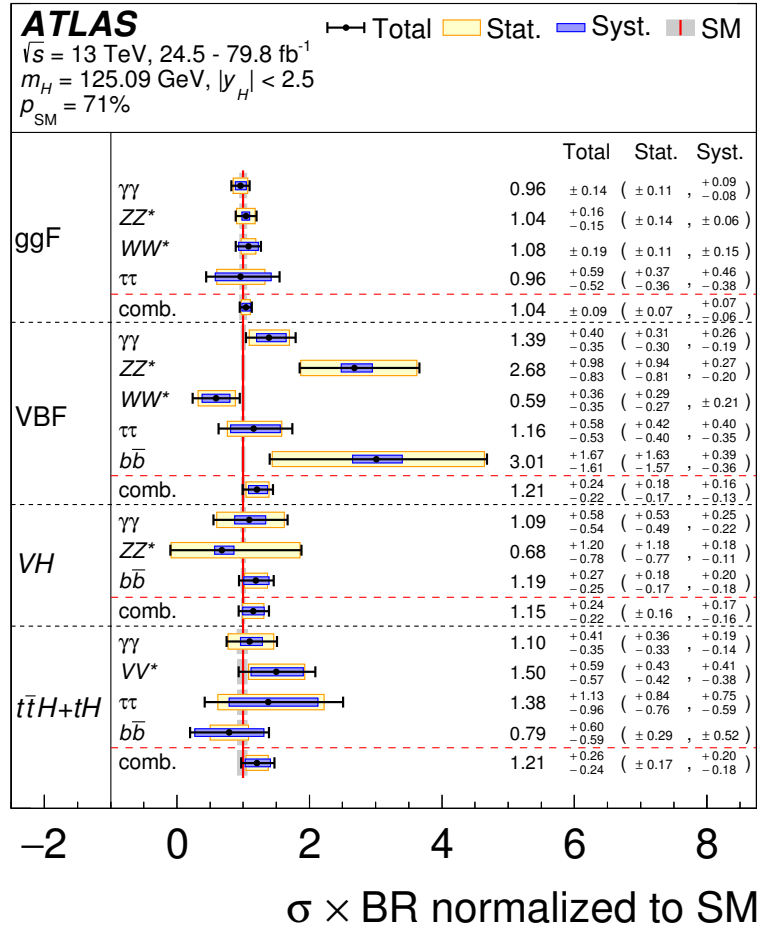


Figure 3: Summary of the measured signal strengths for the production and decay modes studied by the ATLAS Collaboration [10].

These results can be reinterpreted in the context of specific BSM physics models that predict extensions of the scalar sectors, such as the two Higgs doublet model (2HDM) or the minimal supersymmetric SM (MSSM). The precision of the Higgs boson coupling measurements allows to probe broad regions of these models parameter space, as extensively discussed in [10, 11].

#### 4. From observations to precision measurements

The large dataset collected at the LHC Run 2 by the ATLAS and CMS experiments represents a unique opportunity to perform a detailed study of all the Higgs boson production modes, effectively marking a transition from their discovery to the study of their properties. An example is the  $t\bar{t}H$  production, that has been observed in 2018 by the ATLAS and CMS Collaborations [12, 13] with the analysis of the Run 1 and of part of the Run 2 dataset, using a combination of the  $b\bar{b}$ ,  $\gamma\gamma$ ,  $ZZ$ ,  $WW$  and  $\tau\tau$  decay channels. The measured signal strengths are  $1.32^{+0.28}_{-0.26}$  (ATLAS) and  $1.26^{+0.31}_{-0.26}$

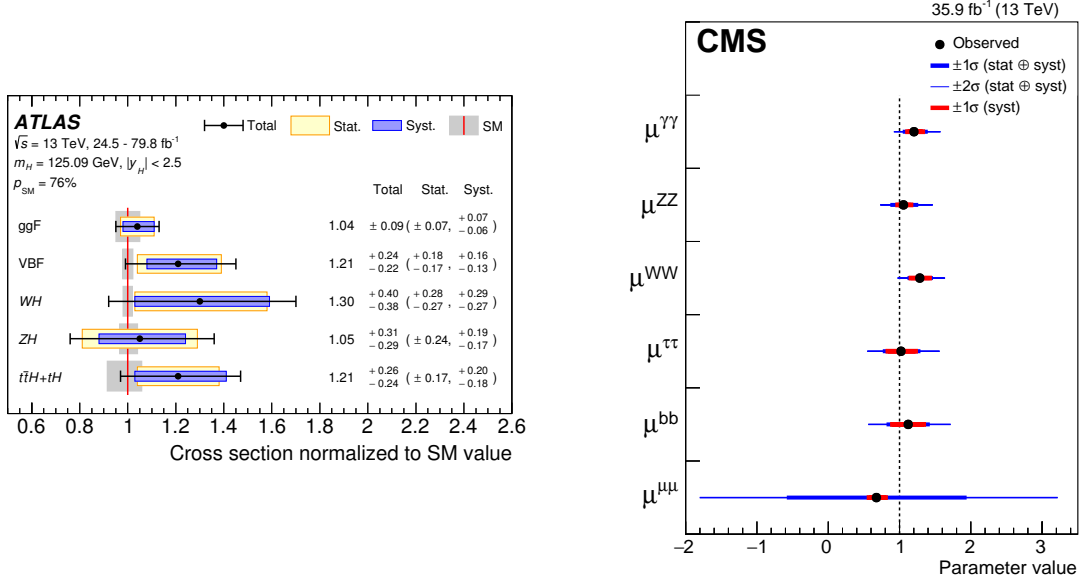


Figure 4: Measured combined signal strengths per production (left, ATLAS Collaboration [10]) and decay mode (right, CMS Collaboration [11]) of the Higgs boson.

(CMS). About one year later, the increase in the size of the available dataset allows us to deepen the understanding of this rare process by studying it with more precision in various decay modes.

The decay mode to two photons is particularly challenging because of the small branching fraction, and thus benefits of the large size of the full Run 2 dataset. The result published by the ATLAS Collaboration [14] achieved almost a single channel observation with an observed (expected) significance of  $4.9\sigma$  ( $4.2\sigma$ ) and a measured signal strength of  $1.38^{+0.41}_{-0.36}$ . The diphoton invariant mass spectrum, that combines all the hadronic and leptonic categories studied in this result, is shown in Fig. 7. Similarly, an updated result by the CMS Collaboration with the 2016 and 2017 datasets [15] sets a value of  $\mu = 1.7^{+0.6}_{-0.5}$ .

The study of  $t\bar{t}H$  in hadronic and multilepton final states benefits of larger branching fractions, but is experimentally challenging because of the complex final states that require the usage of advanced signal identification techniques. As an example, the recent search for  $t\bar{t}H(b\bar{b})$  by the CMS Collaboration [16] uses machine learning methods to reject the abundant multijet and  $t\bar{t}$  background, achieving with the 2016 and 2017 datasets an evidence for this process ( $3.9\sigma$  observed significance and  $3.5\sigma$  expected, with  $\mu = 1.15^{+0.32}_{-0.29}$ ). Similarly, boosted decision trees are used in the study of multilepton final states [17], that targets  $H \rightarrow WW^*$  and  $H \rightarrow \tau\tau$  decays in 7 exclusive categories. An evidence of the  $t\bar{t}H$  process is also achieved with an observed (expected) significance of  $3.2\sigma$  ( $4.0\sigma$ ) and a measured signal strength of  $0.96^{+0.34}_{-0.31}$ . The output of these discriminants in two of the most sensitive categories of the two analyses are shown in Fig. 8.

Similarly to the  $t\bar{t}H$  case, the study of  $H \rightarrow b\bar{b}$  decays has quickly evolved from the observation of this process to its characterisation. The existence of the bottom quark Yukawa coupling has been recently established with a significance larger than  $5\sigma$  by both the ATLAS and CMS Collaborations [18, 19]. The ATLAS Collaboration has recently studied the cross section times branching

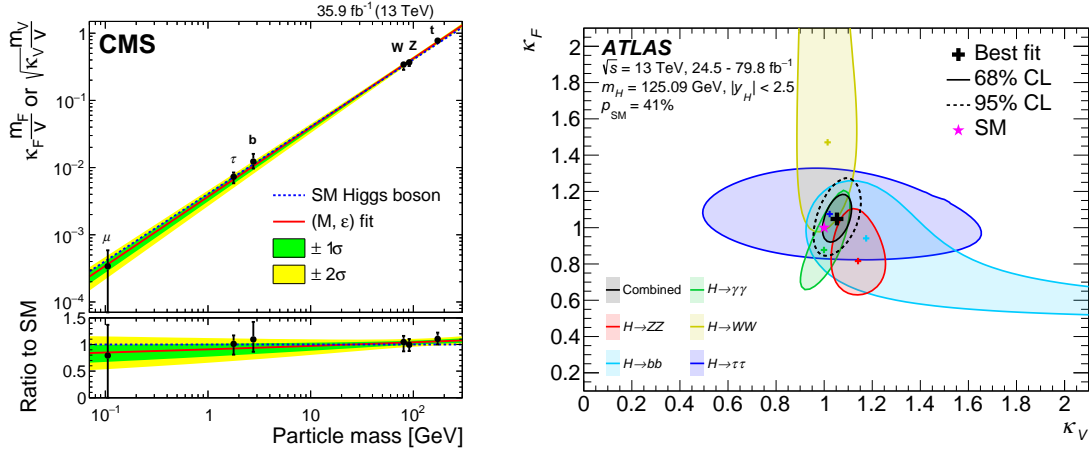


Figure 5: Left: measured values of the coupling modifiers as a function of the particle mass [11]. The ordinate axis reports either the coupling modifier value (for fermions) or its square root (for vector bosons), multiplied by the value of the particle mass and normalised to the vacuum expectation value. Right: measured values of the common coupling modifiers for fermions and vector bosons [10].

fraction of the  $VH(b\bar{b})$  process in exclusive regions of the vector boson  $p_T$  [20]. Sensitivity to the transverse momentum is retained through the shape of the boosted decision tree discriminant that is used to separate the signal from the multijet background, and templates for two (three) intervals of the  $W$  ( $Z$ ) boson  $p_T$  are simultaneously fit to the data. The output of the discriminant and the measured cross sections in bins of the vector boson  $p_T$  are shown in Fig. 9. Good compatibility with the SM predictions is observed within uncertainties.

## 5. Simplified template cross section measurements

With the increasing precision of Higgs boson measurements, the  $\kappa$  framework described in Section 3 does not allow to fully explore the information provided by experimental results. For example, BSM physics may modify specific kinematic region of Higgs boson production such as those with high transverse momentum. However, experimental analyses are often too complex to easily unfold the final result in terms of underlying Higgs boson properties. The simplified template cross section (STXS) framework defines fiducial regions in the phase space of Higgs boson production, allowing to develop sophisticated and optimised analysis methods while ensuring their interpretability, and minimising their dependence on underlying theoretical assumptions. Depending on the statistical power of individual analyses, more granular STXS regions can be defined, and a staged approach has been adopted by experiments. Stage 0 STXS correspond to the individual production modes, while stage 1 corresponds to a further splitting into kinematic regions. An example of STXS measurement is the study of  $VH(b\bar{b})$  production in intervals of the vector bosons  $p_T$  described in Section 4.

The STXS framework allows to develop advanced analysis techniques while providing a theoretically clean and interpretable result. An example is the analysis of the  $H \rightarrow \tau\tau$  process [21],

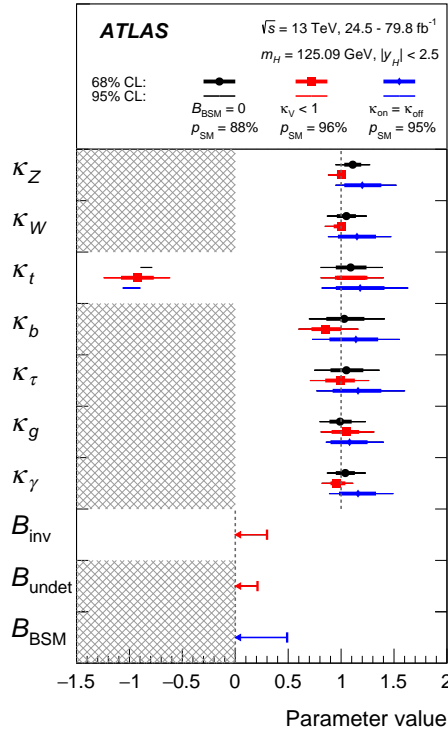


Figure 6: Measured values of the Higgs boson couplings, paramtrising the BSM physics contributions with effective photon and gluon interactions, and with decays to invisible or undetectable particles [10]. The assumptions for the three measurements are discussed in the text.

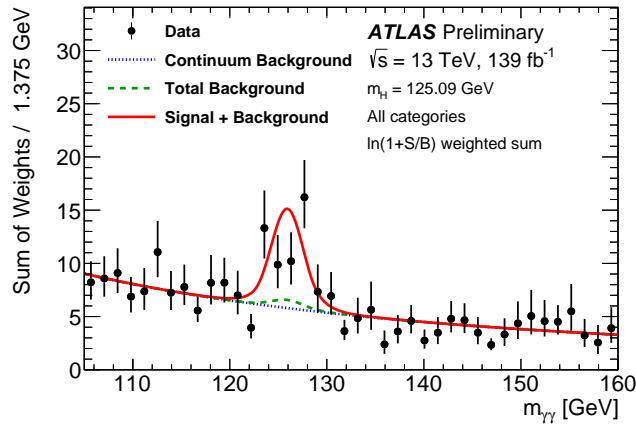


Figure 7: Diphoton invariant mass spectrum observed in the  $t\bar{t}H(\gamma\gamma)$  analysis [14]. Hadronic and leptonic categories are combined.

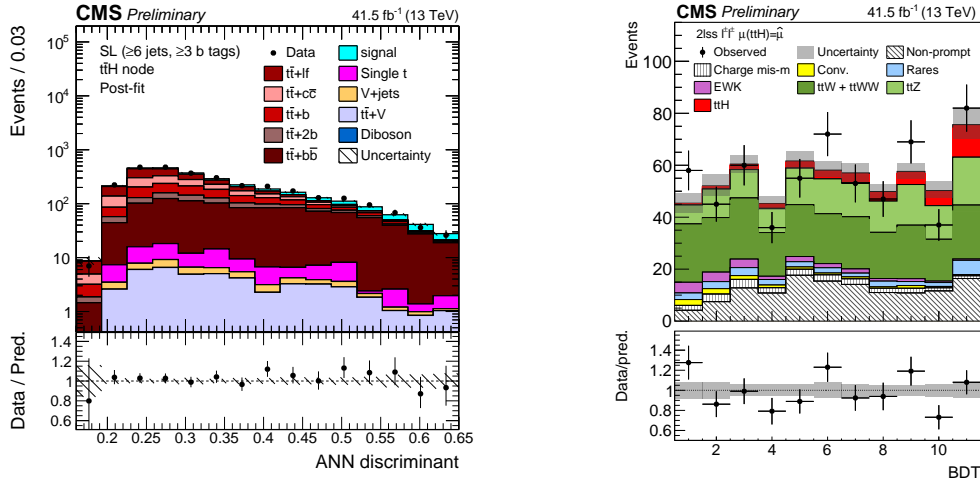


Figure 8: Left: output of the artificial neural network discriminant used in the search for  $t\bar{t}H$  production in the  $H \rightarrow b\bar{b}$  channel [16]. The single lepton category with at least six jets, out of which three identified as  $b$  jets, is shown. Right: output of the boosted decision tree discriminants used in the search for  $t\bar{t}H$  production in the multilepton final state [17]. The category with two leptons with the same electric charge is shown. Each bin corresponds to a region of the bidimensional plane defined by the output of the discriminants trained against  $t\bar{t}$  and  $t\bar{t}V$  production.

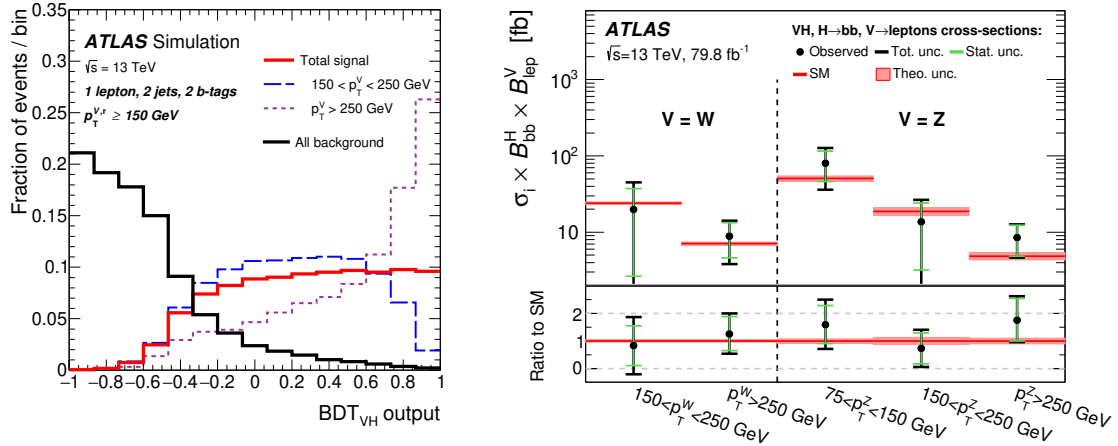


Figure 9: Left: output of the boosted decision tree discriminant used in the  $VH(b\bar{b})$  analysis. Sensitivity to the  $W$  boson  $p_T$  is retained through the distribution of the discriminant. Right: measurement performed in two (three) exclusive intervals of the  $W$  ( $Z$ ) transverse momentum. Both figures are taken from [20].

where the CMS Collaboration has developed sophisticated neural networks with multiprocessing classification to optimally explore four final states of the  $\tau\tau$  system, bringing sensitivity to the gluon and vector boson fusion kinematics. In clean decay channels such as  $H \rightarrow \gamma\gamma$  [22] the granularity of the STXS regions can be improved by further classifying the gluon and vector boson fusion phase space in terms of the kinematics of the Higgs boson and of the jets produced in association. Finally, the STXS approach is designed to be increasingly granular as more data become available. Using the full Run 2 dataset and the clean  $H \rightarrow ZZ^* \rightarrow 4\ell$ , the CMS Collaboration has performed measurements using the so-called stage 1.1 STXS [23], with 10 bins for gluon fusion-like production, 5 bins for vector boson fusion-like production, three bins for VH-like production (with leptonic V decays) and a single bin for  $t\bar{t}H$  and single top quark associated production. The STXS measurements performed by the CMS Collaboration in three final states discussed above are summarised in Fig. 10.

A combined STXS measurements for different channels has been performed by the ATLAS Collaboration [10], as shown in Fig. 11, using the 2016 and 2017 datasets. A general good agreement with the SM prediction is observed within uncertainties. In the regions that are most sensitive to BSM physics contributions, such as those characterised by high transverse momenta, the statistical uncertainty is still the dominant one, and the result is thus expected to be improved further with the analysis of the full Run 2 dataset.

It should be mentioned that fully differential measurements are also performed by the experiments beyond STXS measurements. The CMS Collaboration has performed differential measurements in the four lepton final state using the full Run 2 dataset [23], and the ATLAS Collaboration has performed combined differential measurements in the four lepton and diphoton decay channels with the 2016 dataset [24]. A more extensive discussion of the status of these measurements as of this conference is reported in [25].

## 6. Probing the self-coupling in single Higgs boson measurements

While the Higgs boson self-coupling  $\lambda_{HHH}$  can be directly measured in Higgs boson pair (HH) production, its experimental study in this process is challenging because of the small production cross section and, consequently, Higgs boson self interactions have not yet been observed. Single Higgs boson production provides a complementary access to this elusive coupling thanks to the possibility to perform an indirect measurement, being sensitive to  $\lambda_{HHH}$  through loop-level contributions. These  $\lambda_{HHH}$ -dependent next-to-leading (NLO) electroweak corrections [26, 27] affect both the total Higgs boson production rate and the differential cross sections. Variations are expected in all the main production modes, with the largest effects observed for  $t\bar{t}H$  production. It must be noted that complete differential effects have not yet been computed for gluon fusion, although they are expected to be small [28], therefore only changes in the total cross section are presently investigated in this production mode.

The STXS measurements discussed in Section 5 have been reinterpreted by the ATLAS Collaboration in terms of variations of the Higgs boson self-coupling [29], parametrising the expected change of cross section in each bin of the measurement. The result is shown in Fig. 12, and corresponds to a best fit value of  $\kappa_\lambda = 4.0^{+4.3}_{-4.1}$ , where  $\kappa_\lambda$  is the Higgs boson self coupling value normalised to the SM prediction ( $\kappa_\lambda = \lambda_{HHH}/\lambda_{HHH}^{\text{SM}}$ ). The result assumes that only  $\kappa_\lambda$  can vary,

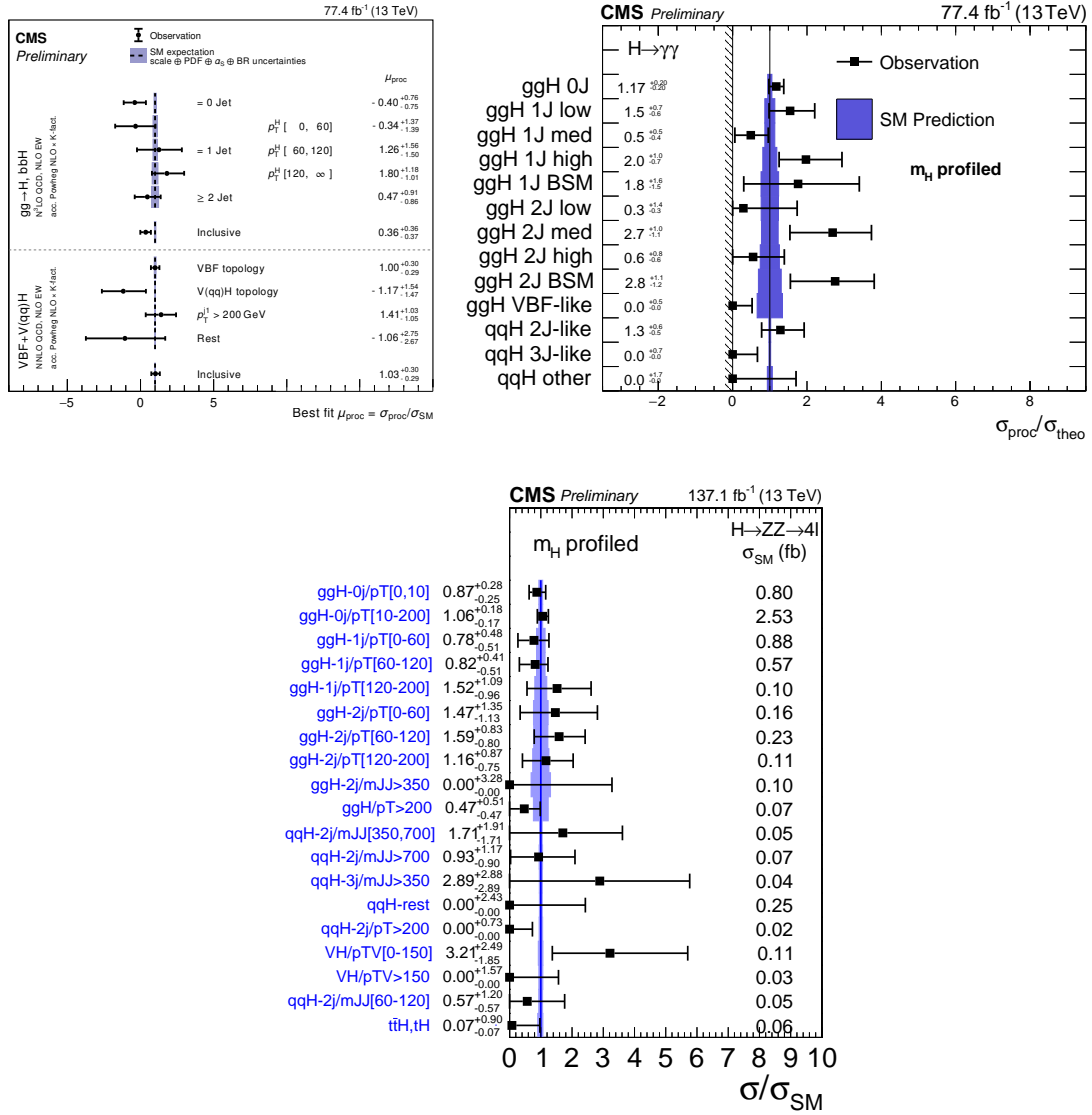


Figure 10: Simplified template cross section measurements performed by the CMS Collaboration in the  $H \rightarrow \tau\tau$  [21] (top left),  $H \rightarrow \gamma\gamma$  [22] (top right), and  $H \rightarrow ZZ^* \rightarrow 4\ell$  [23] (bottom) decay channels.

while all the other couplings are fixed to the SM prediction. If also  $\kappa_V$  is floated, the sensitivity is reduced by about 50%, and no sensitivity is retained when introducing other degrees of freedom in the fit, because the current single Higgs boson measurements do not allow to disentangle variations of  $\kappa_\lambda$  from the effects of other couplings. This can be reduced in future by exploring in more detail the differential information, and by performing a combined measurement with HH results. This combination has been performed by the ATLAS Collaboration after this conference [30], using the same  $\kappa$  framework as the result presented above to combine the leading order  $\kappa_\lambda$  constraint from HH to the loop-level indirect determination from single Higgs measurements.

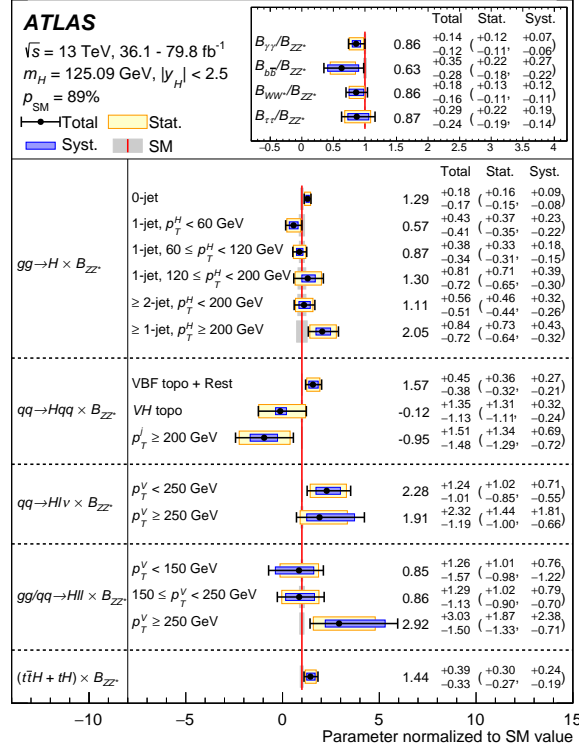


Figure 11: Combined measurement of the STXS performed by the ATLAS Collaboration [10].

## 7. Future prospects

The ultimate precision in the determination of the Higgs boson couplings will be reached at the high-luminosity LHC (HL-LHC), where each experiment is expected to collect a dataset of about  $3000 \text{ fb}^{-1}$ . The high instantaneous luminosity of the HL-LHC, with a number of simultaneous pp interactions per bunch crossing of 140 to 200, represent significant challenges that the experiments are tackling with an ambitious programme of detector upgrade.

The precision in the determination of the Higgs boson couplings has been estimated by extrapolating the current measurements to an integrated luminosity of  $3000 \text{ fb}^{-1}$  per experiment [31]. The performance in object reconstruction efficiencies, misidentification rates and resolutions are assumed to be similar to the LHC Run 2, considering that the detector upgrades will compensate for the harsher collision conditions. Scenarios are defined for the experimental systematic uncertainties, assuming either the same values of the LHC Run 2, or scaling them with the luminosity until a minimal value is reached. Theory uncertainties are generally considered to be reduced by a factor of two. A summary of the projected precision in the Higgs boson couplings measurement with these assumptions is reported in Fig. 13. Most couplings are expected to be measured to a precision ranging between 2 to 4%. The theory uncertainties are the dominant ones in most cases, with the exception of the searches for rare processes such as  $H \rightarrow \mu\mu$  and  $H \rightarrow Z\gamma$ .

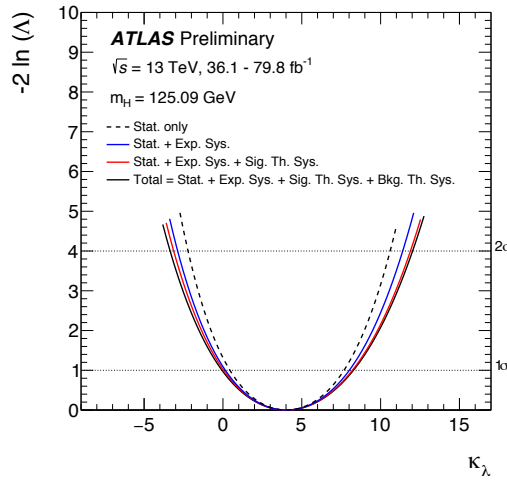


Figure 12: Negative log-likelihood profile as a function of the Higgs boson self coupling modifier from the reinterpretation of single Higgs boson production STXS measurements.

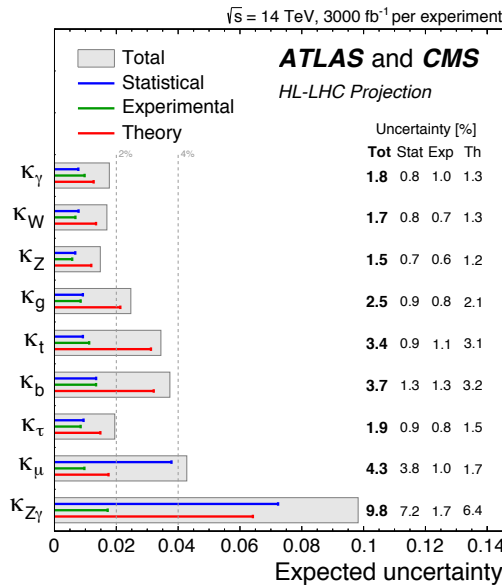


Figure 13: Summary of the projected uncertainties on the Higgs boson couplings measurements at the HL-LHC, combining the ATLAS and CMS results [31]. The red and green lines denote the theory and the experimental systematic uncertainties, while the blue line indicates the statistical ones. The total uncertainty is denoted by the grey box.

## 8. Conclusions

The Higgs boson is a unique particle in Nature, and its thorough characterisation is essential to explore the properties of the scalar sector of the standard model of particle physics. A broad program of measurements is being conducted by the ATLAS and CMS Collaborations, that have studied the Higgs boson mass, width, couplings, and properties. The Run 2 dataset provides an unprecedented opportunity for Higgs boson studies, with the experimental exploration marking a

transition from observations to precision measurements as more data are available. A broad and exciting research program is ahead of the experimental community, from the preparation of updated results using the full Run 2 dataset to the HL-LHC precision measurements.

## References

- [1] F. Englert and R. Brout, “Broken Symmetry and the Mass of Gauge Vector Mesons”, *Phys. Rev. Lett.* **13** (1964) 321, doi:[10.1103/PhysRevLett.13.321](https://doi.org/10.1103/PhysRevLett.13.321).
- [2] P. W. Higgs, “Broken Symmetries and the Masses of Gauge Bosons”, *Phys. Rev. Lett.* **13** (1964) 508, doi:[10.1103/PhysRevLett.13.508](https://doi.org/10.1103/PhysRevLett.13.508).
- [3] ATLAS Collaboration, “The ATLAS Experiment at the CERN Large Hadron Collider”, *JINST* **3** (2008) S08003, doi:[10.1088/1748-0221/3/08/S08003](https://doi.org/10.1088/1748-0221/3/08/S08003).
- [4] CMS Collaboration, “The CMS Experiment at the CERN LHC”, *JINST* **3** (2008) S08004, doi:[10.1088/1748-0221/3/08/S08004](https://doi.org/10.1088/1748-0221/3/08/S08004).
- [5] ATLAS Collaboration, “Measurement of the Higgs boson mass in the  $H \rightarrow ZZ^* \rightarrow 4\ell$  and  $H \rightarrow \gamma\gamma$  channels with  $\sqrt{s} = 13$  TeV  $pp$  collisions using the ATLAS detector”, *Phys. Lett. B* **784** (2018) 345, doi:[10.1016/j.physletb.2018.07.050](https://doi.org/10.1016/j.physletb.2018.07.050), arXiv:[1806.00242](https://arxiv.org/abs/1806.00242).
- [6] CMS Collaboration, “Measurements of properties of the Higgs boson decaying into the four-lepton final state in  $pp$  collisions at  $\sqrt{s} = 13$  TeV”, *JHEP* **11** (2017) 047, doi:[10.1007/JHEP11\(2017\)047](https://doi.org/10.1007/JHEP11(2017)047), arXiv:[1706.09936](https://arxiv.org/abs/1706.09936).
- [7] ATLAS Collaboration, “Constraints on off-shell Higgs boson production and the Higgs boson total width in  $ZZ \rightarrow 4\ell$  and  $ZZ \rightarrow 2\ell 2\nu$  final states with the ATLAS detector”, *Phys. Lett. B* **786** (2018) 223, doi:[10.1016/j.physletb.2018.09.048](https://doi.org/10.1016/j.physletb.2018.09.048), arXiv:[1808.01191](https://arxiv.org/abs/1808.01191).
- [8] CMS Collaboration, “Measurements of the Higgs boson width and anomalous  $HVV$  couplings from on-shell and off-shell production in the four-lepton final state”, *Phys. Rev. D* **99** (2019) 112003, doi:[10.1103/PhysRevD.99.112003](https://doi.org/10.1103/PhysRevD.99.112003), arXiv:[1901.00174](https://arxiv.org/abs/1901.00174).
- [9] CMS Collaboration, “Limits on the Higgs boson lifetime and width from its decay to four charged leptons”, *Phys. Rev. D* **92** (2015) 072010, doi:[10.1103/PhysRevD.92.072010](https://doi.org/10.1103/PhysRevD.92.072010), arXiv:[1507.06656](https://arxiv.org/abs/1507.06656).
- [10] ATLAS Collaboration, “Combined measurements of Higgs boson production and decay using up to  $80 \text{ fb}^{-1}$  of proton-proton collision data at  $\sqrt{s} = 13$  TeV collected with the ATLAS experiment”, arXiv:[1909.02845](https://arxiv.org/abs/1909.02845).
- [11] CMS Collaboration, “Combined measurements of Higgs boson couplings in proton–proton collisions at  $\sqrt{s} = 13$  TeV”, *Eur. Phys. J. C* **79** (2019) 421, doi:[10.1140/epjc/s10052-019-6909-y](https://doi.org/10.1140/epjc/s10052-019-6909-y), arXiv:[1809.10733](https://arxiv.org/abs/1809.10733).
- [12] ATLAS Collaboration, “Observation of Higgs boson production in association with a top quark pair at the LHC with the ATLAS detector”, *Phys. Lett. B* **784** (2018) 173, doi:[10.1016/j.physletb.2018.07.035](https://doi.org/10.1016/j.physletb.2018.07.035), arXiv:[1806.00425](https://arxiv.org/abs/1806.00425).
- [13] CMS Collaboration, “Observation of  $t\bar{t}H$  production”, *Phys. Rev. Lett.* **120** (2018) 231801, doi:[10.1103/PhysRevLett.120.231801](https://doi.org/10.1103/PhysRevLett.120.231801), arXiv:[1804.02610](https://arxiv.org/abs/1804.02610).
- [14] ATLAS Collaboration, “Measurement of Higgs boson production in association with a  $t\bar{t}$  pair in the diphoton decay channel using  $139\text{-fb}^{-1}$  of LHC data collected at  $\sqrt{s} = 13\text{-TeV}$  by the ATLAS experiment”, Conference note ATLAS-CONF-2019-004, CDS ID: 2668103, 2019.

- [15] CMS Collaboration, “Measurement of the associated production of a Higgs boson and a pair of top-antitop quarks with the Higgs boson decaying to two photons in proton-proton collisions at  $\sqrt{s} = 13\text{ TeV}$ ”, Physics Analysis Summary CMS-PAS-HIG-18-018, CDS ID: 2649208, 2018.
- [16] CMS Collaboration, “Measurement of  $t\bar{t}H$  production in the  $H \rightarrow b\bar{b}$  decay channel in  $41.5\text{ fb}^{-1}$  of proton-proton collision data at  $\sqrt{s} = 13\text{ TeV}$ ”, Physics Analysis Summary CMS-PAS-HIG-18-030, CDS ID: 2675023, 2019.
- [17] CMS Collaboration, “Measurement of the associated production of a Higgs boson with a top quark pair in final states with electrons, muons and hadronically decaying  $\tau$  leptons in data recorded in 2017 at  $\sqrt{s} = 13\text{ TeV}$ ”, Physics Analysis Summary CMS-PAS-HIG-18-019, CDS ID: 2649199, 2018.
- [18] ATLAS Collaboration, “Observation of  $H \rightarrow b\bar{b}$  decays and  $VH$  production with the ATLAS detector”, *Phys. Lett. B* **786** (2018) 59, doi:10.1016/j.physletb.2018.09.013, arXiv:1808.08238.
- [19] CMS Collaboration, “Observation of Higgs boson decay to bottom quarks”, *Phys. Rev. Lett.* **121** (2018) 121801, doi:10.1103/PhysRevLett.121.121801, arXiv:1808.08242.
- [20] ATLAS Collaboration, “Measurement of  $VH$ ,  $H \rightarrow b\bar{b}$  production as a function of the vector-boson transverse momentum in 13 TeV pp collisions with the ATLAS detector”, *JHEP* **05** (2019) 141, doi:10.1007/JHEP05(2019)141, arXiv:1903.04618.
- [21] CMS Collaboration, “Measurement of Higgs boson production and decay to the  $\tau\tau$  final state”, Physics Analysis Summary CMS-PAS-HIG-18-032, CDS ID: 2668685, 2019.
- [22] CMS Collaboration, “Measurements of Higgs boson production via gluon fusion and vector boson fusion in the diphoton decay channel at  $\sqrt{s} = 13\text{ TeV}$ ”, Physics Analysis Summary CMS-PAS-HIG-18-029, CDS ID: 2667225, 2019.
- [23] CMS Collaboration, “Measurements of properties of the Higgs boson in the four-lepton final state in proton-proton collisions at  $\sqrt{s} = 13\text{ TeV}$ ”, Physics Analysis Summary CMS-PAS-HIG-19-001, CDS ID: 2668684, 2019.
- [24] ATLAS Collaboration, “Combined measurement of differential and total cross sections in the  $H \rightarrow \gamma\gamma$  and the  $H \rightarrow ZZ^* \rightarrow 4\ell$  decay channels at  $\sqrt{s} = 13\text{ TeV}$  with the ATLAS detector”, *Phys. Lett. B* **786** (2018) 114, doi:10.1016/j.physletb.2018.09.019, arXiv:1805.10197.
- [25] J. Adelman on behalf of the ATLAS and CMS Collaborations, “Differential Higgs (EW interpretation) and diboson cross sections at ATLAS and CMS”, *PoS (LHCP2019) 102*. This conference.
- [26] G. Degrandi, P. P. Giardino, F. Maltoni, and D. Pagani, “Probing the Higgs self coupling via single Higgs production at the LHC”, *JHEP* **12** (2016) 080, doi:10.1007/JHEP12(2016)080, arXiv:1607.04251.
- [27] F. Maltoni, D. Pagani, A. Shivaji, and X. Zhao, “Trilinear Higgs coupling determination via single-Higgs differential measurements at the LHC”, *Eur. Phys. J.* **C77** (2017) 887, doi:10.1140/epjc/s10052-017-5410-8, arXiv:1709.08649.
- [28] M. Gorbahn and U. Haisch, “Two-loop amplitudes for Higgs plus jet production involving a modified trilinear Higgs coupling”, *JHEP* **04** (2019) 062, doi:10.1007/JHEP04(2019)062, arXiv:1902.05480.
- [29] ATLAS Collaboration, “Constraint of the Higgs boson self-coupling from Higgs boson differential production and decay measurements”, ATLAS note ATL-PHYS-PUB-2019-009, CDS ID: 2667570, 2019.

- [30] ATLAS Collaboration, “Constraints on the Higgs boson self-coupling from the combination of single-Higgs and double-Higgs production analyses performed with the ATLAS experiment”, ATLAS Conference Note ATLAS-CONF-2019-049, CDS ID: 2693958, 2019.
- [31] HL/HE WG2 group Collaboration, “Higgs Physics at the HL-LHC and HE-LHC”, [arXiv:1902.00134](https://arxiv.org/abs/1902.00134).